Micromachining along a curve: femtosecond laser micromachining of curved profiles in diamond and silicon using accelerating beams

A. Mathis, F. Courvoisier, L. Froehly, L. Furfaro,

M. Jacquot, P. A. Lacourt and J. M. Dudley

Département d'Optique P.M. Duffieux, Institut FEMTO-ST,

UMR 6174 CNRS Université de Franche-Comté, 25030 Besançon Cedex, France

francois.courvoisier@femto-st.fr

Abstract

We report femtosecond laser micromachining of micron-size curved structures using tailored accelerating beams. We report surface curvatures as small as 70 μm in both diamond and silicon, which demonstrates the wide applicability of the technique to materials that are optically transparent or opaque at the pump laser wavelength. We also report the machining of curved trenches in silicon. Our results are consistent with an ablation-threshold model based on calculated local beam intensity, and we also observe asymmetric debris deposition which is interpreted in terms of the optical properties of the incident accelerating beam.

The use of high power lasers for material ablation is widely applied in a broad range of technologies in material processing[1]. With appropriate selection of laser wavelength, power and pulse duration, many impressive examples of both surface and volumetric processing in a variety of materials have been developed, at scales from centimeters to nanometers.[2-4] A particular challenge in laser material processing, however, is machining structures both at the surface and within the sample that have longitudinally-varying characteristics, because this requires simultaneous control of beam steering and sample rotation and translation. This becomes especially difficult when the desired spatial features have micron or sub-micron scale.[5]

In this paper, we present a solution to this problem using accelerating femtosecond laser beams to machine both curved surface profiles and curved trenches on micron scales. For diamond and silicon samples, we machine initially square sample edges to curved circular profiles, and we also show experimental results in silicon where accelerating beams have been applied to writing curved trenches to ~ 80 μm depth within the bulk sample. In fact, although our experiments have been performed in the femtosecond regime, accelerating beams can be generated with laser beams of any temporal duration (even continuous wave). Our results therefore extend the technology of laser material processing into a regime where curved features are generated from the intrinsic properties of the laser beam itself rather than as a result of geometric sample rotation.

Accelerating beams are a class of laser beam that consist of a strongly-localized high intensity lobe that follows a propagation trajectory that displays curvature in a dimension transverse to its propagation. Since their experimental demonstration in 2007,[6] accelerating beams have been applied to particle sorting and nonlinear optics,[7,8] and they have recently

attracted much attention as it has been shown that they represent a fundamentally original class of solution to Maxwell's equations for spatial beam propagation[9,10] and that they represent a stationary solution in the nonlinear regime.[11] They can be readily synthesized from a Gaussian laser beam through the application of an appropriate spatial phase function, and their properties can be interpreted usefully in terms of the properties of optical caustics.[10,12-16]

In our experiments, we generate accelerating beams from a 5 kHz amplified Ti:Sapphire laser emitting 100 fs pulses at a central wavelength of 800 nm, by applying appropriate spatial phase to the Gaussian laser beam using an optically-addressed spatial light modulator (SLM). We design a phase profile to generate an accelerating laser beam in the form of a primary high intensity lobe that takes the form of a curved cylinder or tube as it propagates. Our phase mask design uses the combination of two 1-dimensional masks at 90 degrees.[6] The phase masks were designed in order to produce an accelerating beam in the first order of diffraction of our SLM. An imaging system is used to place the Fourier-filtered image of the SLM phase profile at the back focal plane of a high numerical aperture (NA 0.8) microscope objective, as shown on figure 1(a). The accelerating beam with main intensity lobe transverse dimensions of ~2 μm is produced in the focal region of the microscope objective. The 3D surface of isointensity at half-maximum which highlights the primary lobe only is shown in red in figure 1(a). To aid in the visualization of the complete spatial field profile, the figure on the right plots the isosurface at 5% of the maximal intensity at a viewing angle selected to illustrate the acceleration profiles of the subsidiary lobes of the Airy functions.

Figure 1(b) shows experimental measurements of the beam profile along the propagation direction in the *xz* plane (side view) and in the *xy* plane (top view). This particular accelerating beam corresponds to a target circular trajectory of radius R = 120 μm, shown as a white curve. The top view shows the measured transverse profile at $z = 0$, and the beam

properties are well-fitted by two dimensional Airy functions perpendicular to each other, i.e. $\left|Ai\left(\alpha(x-y)\right)Ai\left(\alpha(x+y)\right)\right|^2$ with central lobe FWHM of ~2 μm. Note that even though Airy functions correspond strictly only to paraxial and parabolic accelerating trajectories, they have in fact been shown to provide an accurate description of the main intensity lobe characteristics for arbitrary acceleration profiles even in the non-paraxial regime.[10,17,18]

The high intensity accelerating tube separates two regions: on the outside of the circle, there is subsidiary structure corresponding to the Airy function minima, while on the inside there is a shadow zone of zero intensity. This structure naturally suggests application in machining convex surfaces which is the case considered here. As shown in figure 1(a), we position the sample profile in the plane of the beam acceleration so that the high intensity tube is the first area of the beam that encounters the surface to be machined. It is this part of the beam that therefore induces ablation, while the other lobes of the beam freely propagate outside the sample.

Sample positioning was performed by visualization through the focusing microscope objective on a CCD camera as in reference 19. Samples were placed on a gimbal mount to ensure planarity better than 1 mrad, and positioned using a motorized stepping motor with 100 nm resolution. In the back focal plane of the microscope objective, the beam polarization is parallel to x axis, but the polarization of the accelerating beam in the vicinity of the main intensity lobe is in the xz plane perpendicular to the beam trajectory. The pulse duration was 120 fs at the sample site.

We have applied this approach to machine curved surfaces of sample materials that were both transparent and opaque at the 800 nm pump wavelength used. For transparent materials, we selected diamond slides, and for the opaque material, we used silicon wafers. A selection of results is shown in Fig. 2. Scanning electron micrograph (SEM) images of the

results obtained for diamond are shown in Fig. 2(a), where we machined a circular profile of 70 μm radius on a diamond slide of 50 μm thickness. The process used here consisted of moving the sample into the 11 μJ energy beam in 0.3 μm steps along the x-direction, and machining at each position with one (back and forth) pass along the edge at a translation speed 10 μm/s. Results for silicon are shown in Fig. 2(b). The higher ablation rate for silicon[20] allowed translation using larger steps of 0.5 μm while the other parameters were kept identical.

It is easy to confirm from the SEM images that the curved profiles in both diamond and silicon are in quantitative agreement with the trajectory of the main intensity lobe. In particular, the precise shapes of the machined profiles are determined by the form of the beam profile that follows the fluence isocontour at the ablation threshold. Indeed, the bottom images in Fig. 2 show a side view of the SEM images of the samples to permit a quantitative comparison with the threshold fluence isocontour profile for each material (~1.1 J/cm^2 for diamond[21] and ~1J/cm^2 for silicon[20]). There is clearly excellent visual agreement; more detailed analysis shows that the machined surface follows the beam contour to within ±0.5 μm. The processed surfaces exhibited roughness on the order of 200 nm (diamond) and 500 nm (silicon) with no evidence of deleterious structures such as cracks or voids.

We also investigated the possibility of using the accelerating beams directly incident upon the surface in order to machine curved trenches within a sample. Figure 3 shows the SEM images of trenches machined in a 100 μm thick silicon sample using a 120 μm radius beam. In Fig. 3(a) we show results at fixed energy of 11 μJ/pulse using a sample translation of 100 μm/s as a function of increasing (back and forth) passes along a 4 mm line. The sample was diced before imaging. It is clear that the machining process evolves downwards into the sample from the surface, and that trench depth increases with the number of passes.

Significantly, we see that the debris deposition using the accelerating beam is highly asymmetric, with debris mainly redeposited on the surface of the sample away from the position of the primary intensity lobe. A possible explanation for this could be that the ablated plume is directed perpendicular to the ablated surface itself [22], and we anticipate that this phenomenon could be advantageous in applications such as laser dicing. In Fig. 3(b) we show similar results but studying the variation of trench properties as a function of energy with a fixed number of passes. With this side view, we also compare the form of the machined trenches with the profile of the accelerating beam (dashed line) and we see excellent agreement.

In conclusion, we have shown in this paper how accelerating beams can be used for ultrafast laser processing of curved profiles in transparent and opaque materials, applied to both surface processing and trench machining. Although our results have been obtained using femtosecond pulses where the thermally affected zone is reduced compared to laser processing techniques using longer pulses, the essential approach introduced here is applicable more widely provided that the thermally affected zone is smaller than the curvature of the target trajectory. We anticipate a broad range of applications in different technological fields such as the processing of flat panels and precision photonic components

Acknowledgements: The authors thank B. Guichardaz, L. Gauthier-Manuel and R. Salut for important technical assistance. We acknowledge funding from the Région of Franche-Comté and the Agence Nationale de la Recherche, contracts 2011-BS04-010-01 NANOFLAM, 2011-BS09-026-02-SMART_LASIR, ANR-09-BLAN-0065 IMFINI.

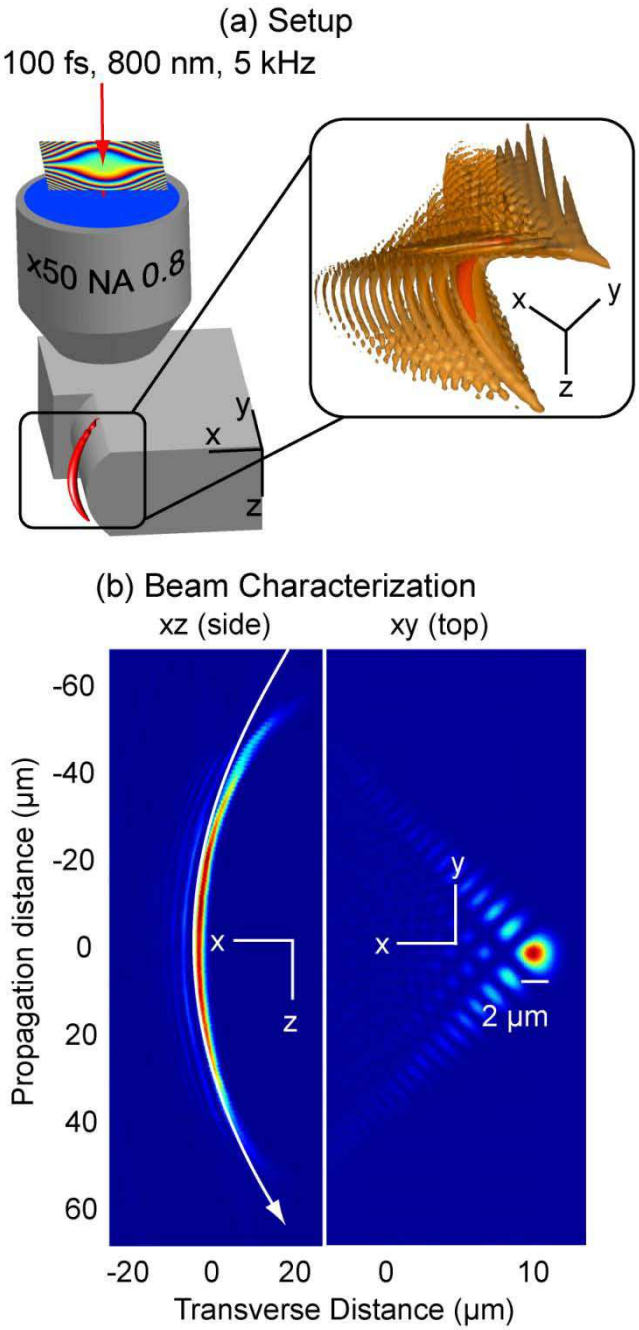

Figure 1: (a) Schematic of our experimental setup showing focusing of shaped accelerating beam into our sample. (b) Experimental measurements of accelerating beam profile along direction of propagation i.e. the xz plane in a side view, and viewed from the top in the xy plane at the point of peak intensity at z = 0. The white line shows the target circular beam trajectory with radius R=120 μm.

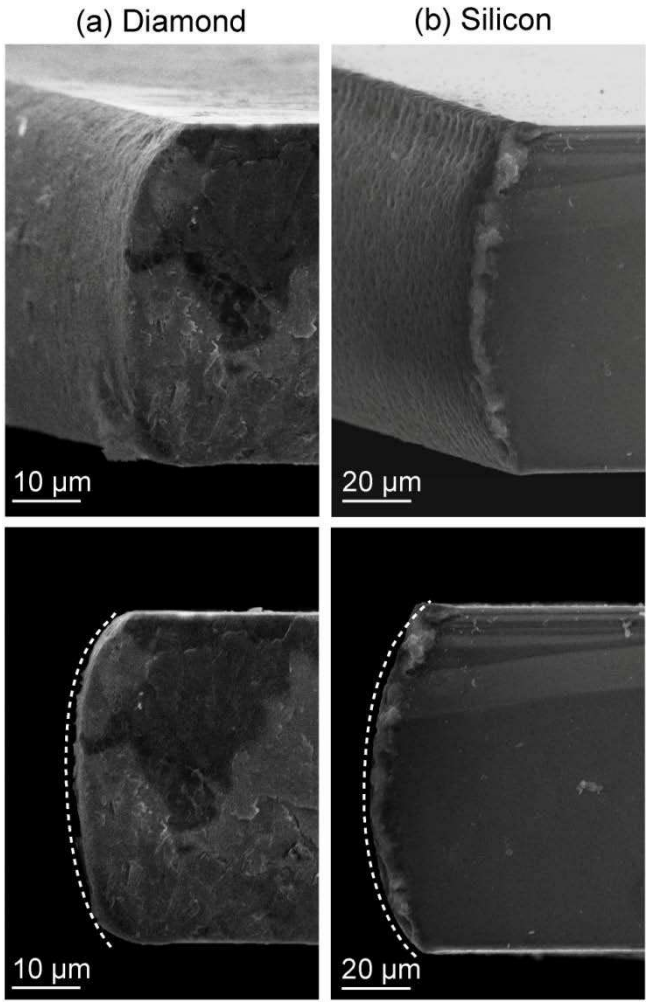

Figure 2: Machining of (a) diamond and (b) silicon using circular accelerating beams. Top row subfigures show 3D view, bottom row subfigures show images with the sample oriented for quantitative profile measurements. In (a) the profile (beam) radius is 70 μm and the sample thickness is 50 μm. In (b) the profile (beam) radius is 120 μm and the sample thickness is 100 μm. In the bottom row we compare the form of the machined surface with the expected profile using the calculated ablation threshold fluence isocontour.

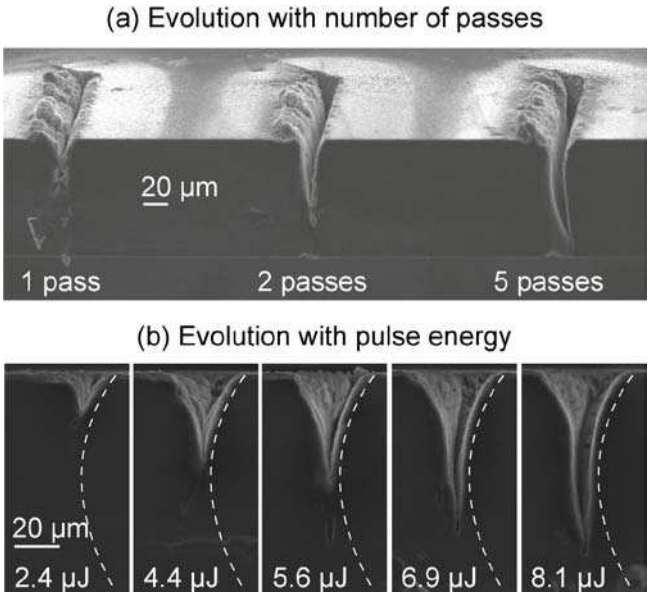

Figure 3: Machining of curved trenches in silicon using accelerating beams. In (a) we show the variation in trench properties for different number of passes at fixed energy of 11 µJ. In (b) we use a fixed number of 5 passes and study the variation in the trench properties with incident energy.

References

[1] C. R. Phipps, *Laser Ablation And Its Applications* (Springer, New York, 2007)
[2] P. P. Pronko, S. K. Dutta, J. Squier, J. V. Rudd, D. Du, G. Mourou, Opt. Commun. **114**, 106 (1995)
[3] R. R. Gattass and E. Mazur, Nat. Photonics **2**, 219 (2008).
[4] M.K. Bhuyan, F. Courvoisier, P.-A. Lacourt, M. Jacquot, R. Salut, L. Furfaro, and J. M. Dudley, Appl. Phys. Lett. **97**, 081102 (2010).
[5] A. Ancona, D. Nodop, J. Limpert, S. Nolte, and A. Tünnermann, Appl. Phys. A **94**, 19 (2008).
[6] G.A. Siviloglou, J. Broky, A. Dogariu, and D.N. Christodoulides, Phys. Rev. Lett. **99**, 213901 (2007).
[7] J. Baumgartl, M. Mazilu, K. Dholakia, Nat. Photonics **2**, 675-678 (2008)
[8] P. Polynkin, M. Kolesik, J. V. Moloney, G, A. Siviloglou, D. N. Christodoulides, Science **324**, 229 (2009).
[9] I. Kaminer, R. Bekenstein, J. Nemirovsky, and M. Segev, Phys. Rev. Lett. **108**, 163901 (2012).
[10] F. Courvoisier, A. Mathis, L. Froehly, R. Giust, L. Furfaro, P. A. Lacourt, M. Jacquot, J. M. Dudley, Opt. Lett. **37**, 1736 (2012).
[11] A. Lotti, D. Faccio, A. Couairon, D. Papazoglou, P. Panagiotopoulos, D. Abdollahpour, and S. Tzortzakis, Phys. Rev. A 84, 1-4 (2011).
[12] L. Froehly, F. Courvoisier, A. Mathis, M. Jacquot, L. Furfaro, R. Giust, P. A. Lacourt, J. M. Dudley, Opt. Express **19**, 16455 (2011).
[13] E. Greenfield, M. Segev, W. Walasik, O. Raz, Phys. Rev. Lett. **106**, 213902 (2011).
[14] D. G. Papazoglou, S. Suntsov, D. Abdollahpour, S. Tzortzakis, Phys. Rev. A **81**, 061807 (2010).
[15] Y. Kaganovsky and E. Heyman, Opt. Express **18**, 8440 (2010).
[16] I. D. Chremmos, Z. Chen, D. N. Christodoulides, N. K. Efremidis, Phys. Rev. A **85**, 023828 (2012).
[17] Y. Kaganovsky and E. Heyman, J. Opt. Soc. Am. B **29**, 671 (2012).
[18] R. Gilmore, *Catastrophe theory for scientists and engineers* (Dover, New York,1993).
[19] F. Courvoisier, P. Lacourt, M. Jacquot, M. K. Bhuyan, L. Furfaro, J. M. Dudley, Opt. Lett. **34**, 3163 (2009).
[20] T. H. R. Crawford, A. Borowiec, H. K. Haugen, Appl. Phys. A. **80**, 1717 (2005).
[21] T. V. Kononenko, M. Meier, M. S. Komlenok, S. M. Pimenov, V. Romano, V. P. Pashinin, V. I. Konov, Appl. Phys. A **90**, 645 (2008).
[22] David B. Geohegan, Appl. Phys. Lett. **60**, 2732 (1992).